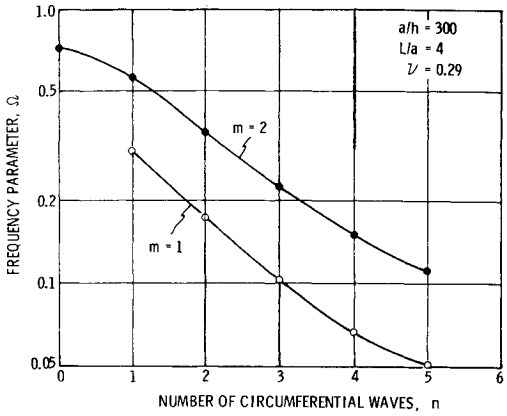

Fig. 1 Frequency distribution for clamped steel shell.

used to compute these constants,[7] usually the constants will form mode shapes that are complex functions. It follows from the nature of the solution that, in the complex plane, all these initial mode shape functions lie on a straight line that passes through the origin. Thus each complex quantity is related to its real component by an identical constant of proportionality, and, since we are accustomed to working with real displacements, it is convenient (and valid) to use these proportional real components (normalized as desired) as the shell's orthogonal mode shapes.

Results and Conclusions

Natural frequencies for the first six circumferential wave numbers and the two lowest radial modes are presented in Table 1 for a clamped-clamped steel shell with $L = 12$ in., $a = 3$ in., and $h = 0.01$ in. Comparisons are made in Table 1 with theoretical results for $n \geqq 1$ that were obtained for the same shell in Refs. 3 and 4. These earlier results are from solutions to Flügge's equations that were computed only after using the uncoupling conditions suggested by Yu.[8] The variation in the frequency parameter for this case is illustrated in Fig. 1. Of particular interest is the spatial phase shift in Fig. 2 between the lowest frequency radial modes for $n = 0$ and for $n \geqq 1$.

The technical significance of this shift lies in the fact that for $n = 0$, the lowest frequency radial mode actually is antisymmetric ($m = 2$) and thus cannot respond to a uniform radial blast load. This important result agrees with Ref. 6 but is in contrast to a misconception which might easily arise from earlier work and in particular the monograph of Ref. 9. The misconception is that the lowest mode of a clamped shell with $n = 0$ is symmetric ($m = 1$). Although the correct situation was noted by Forsberg[2] in his analysis of the axisymmetric vibration of a clamped shell the proper interpretation that $m = 2$ is lacking in recent publications such as Ref. 9.

Table 1 Frequencies (Hz) for clamped shell[a]

m	Source	n					
		0	1	2	3	4	5
1	Present		3425	1917	1153	762	575
	Ref. 3		3423	1917	1154	765	581
	Ref. 4		3427	1918	1145	765	580
2	Present	8017	6412	3903	2536	1751	1284
	Ref. 3		6412	3903	2536	1752	1287
	Ref. 4		6423	3905	2538	1753	1287

[a] $L = 12.0$ in., $a = 3.0$ in., $h = 0.01$ in., $E = 29.6 \times 10^6$ psi, $\nu = 0.29$, $\rho = 0.733 \times 10^{-3}$ lb.-sec^2/in.[4]

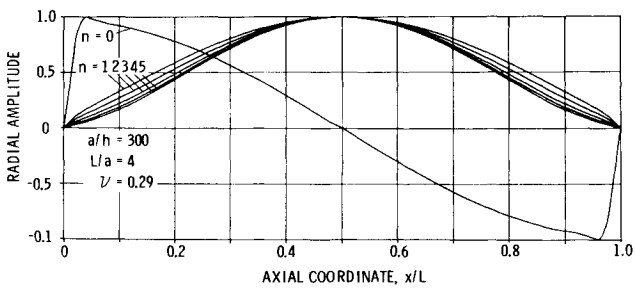

Fig. 2 Initial radial mode shape for clamped steel shell.

References

[1] Forsberg, K., "Influence of Boundary Conditions on the Modal Characteristics of Thin Cylindrical Shells," *AIAA Journal*, Vol. 2, No. 12, Dec. 1964, pp. 2150–2167.

[2] Forsberg, K., "Axisymmetric and Beam-Type Vibrations of Thin Cylindrical Shells," *AIAA Journal*, Vol. 7, No. 2, Feb. 1969, pp. 221–227.

[3] Smith, B. L. and Haft, E. E., "Natural Frequencies of Clamped Cylindrical Shells," *AIAA Journal*, Vol. 6, No. 4, April 1968, pp. 720–721.

[4] Vronay, D. F. and Smith, B. L., "Free Vibrations of Circular Cylindrical Shells of Finite Length," *AIAA Journal*, Vol. 8, No. 3, March 1970, pp. 601–603.

[5] Flügge, W., *Stresses in Shells*, Springer-Verlag, Berlin, 1962.

[6] El Raheb, M. S., "Some Approximations in the Dynamic Shell Equations," Ph.D. thesis, 1970, California Institute of Technology, Pasadena, Calif.

[7] Rubinstein, M. F., *Structural Systems-Statics, Dynamics and Stability*, Prentice-Hall, Englewood Cliffs, N.J., 1970, pp. 20–21.

[8] Yu, Y. Y., "Free Vibrations of Thin Cylindrical Shells Having Finite Lengths with Freely Supported and Clamped Edges," *Journal of Applied Mechanics*, Vol. 77, 1955, pp. 547–552.

[9] Leissa, A. W., *Vibration of Shells*, NASA SP-288, 1973, pp. 87–113.

Nonlinear Creep Analysis by Assumed Stress Finite Element Methods

T. H. H. PIAN*
MIT, Cambridge, Mass.

I. Introduction

FINITE element methods for analyzing the creep behavior of structures have been introduced by many authors.[1-8] They are invariably incremental elastic solutions by direct stiffness methods derived by the conventional assumed displacement approach and based on equivalent nodal forces due to the creep strains that are anticipated during each time increment. When the incremental solutions are carried out without iteration, they are analogous to the Euler's method for numerical integration of differential equations and hence require very small time increments. Indeed, numerical instability for such analysis has been experienced by some investigators when the time increments are not kept sufficiently small.[5] In many available computing codes, the incremental solutions are accompanied by iterative schemes.[7]

Received April 11, 1974. This work was sponsored by the Air Force Office of Scientific Research under Contract F44620-72-C-0018.

Index category: Thermal Stresses.

* Professor of Aeronautics and Astronautics. Associate Fellow AIAA.

The present Note presents an alternative approach based on assumed stress finite element models. In the case of steady-state creep or of transient creep under a time-hardening rule, the finite element formulation leads to a system of first-order nonlinear differential equations which can be solved by using many efficient numerical schemes in either one-step methods such as the various Runge-Kutta methods or multistep methods such as the various versions of the predictor-corrector method.

A variational theorem for creep based on the Hellinger-Reissner principle was developed[9,10] and applied to the formulation of approximate solutions for large deflection and buckling problems involving creep strains.[9,11] Thus it is natural to extend such variational theorem to the finite element formulation of creep problems. The presente Note is limited to the small deflection theory. The corresponding finite-element model is the mixed model which involves independently assumed displacements and stresses.[12] The so-called assumed stress hybrid model may be interpreted as a mixed model based on assumed equilibrating stresses and on assumed displacements along the element boundary; hence it can also be employed to formulate the creep problems.

It is realized that a typical problem associated with creep of metals involves time independent plastic behavior. The assumed stress hybrid model has been demonstrated to be a practical scheme for analyzing elastic-plastic behavior.[13] Thus it can be used to formulate a combined elastic-plastic and creep problem. For simplicity, however, the present discussion is limited to nonlinear creep with linear elastic behavior.

II. Variational Principles for Creep

When a solid continuum is subdivided into finite number of elements, the Hellinger-Reissner principle for the creep problem is $\delta\pi_R = 0$, where

$$-\pi_R = \sum_n \{\int_{V_n}[(1/2)S_{ijkl}\dot{\sigma}_{ij}\dot{\sigma}_{kl} - (1/2)\dot{\sigma}_{ij}(\dot{u}_{i,j}+\dot{u}_{j,i}) + \dot{\varepsilon}_{ij}{}^c\dot{\sigma}_{ij} + \dot{\bar{F}}_i\dot{u}_i]\,dV + \int_{S_{\sigma_n}}\dot{\bar{T}}_i\dot{u}_i\,dS + \int_{S_{u_n}}\dot{T}_i(\dot{u}_i-\dot{\bar{u}}_i)\,dS\} \quad (1)$$

σ_{ij} is the stress tensor; u_i, the displacement vector; $\dot{\varepsilon}_{ij}{}^c$, the rate of creep strain which may be expressed as a function of stress and time; S_{ijkl}, the elastic compliance tensor; F_i, the body force components; T_i, the surface traction; V_n, the volume of the nth element; S_{u_n}, the boundary of V_n where displacements are prescribed; and S_{σ_n}, the boundary of V_n where surface tractions are prescribed. The symbol ($\dot{}$) represents time derivatives; ($\bar{}$) is used to indicate prescribed quantities. It is realized that in applying this variational principle for a finite element formulation it is not necessary to maintain the stress continuity along the interelement boundary if the displacement compatibility is maintained. In the ordinary linear elastic analysis, the Hellinger-Reissner principle can lead to a matrix mix method if both nodal displacements and nodal stresses are left as unknowns in the global matrix equations. This principle can also lead to a matrix displacement method if the stress parameters are independent for different elements hence can be eliminated at the element level.

When the stresses satisfy the equations of equilibrium, the variational principle becomes a modified complementary energy principle; i.e., $\delta\pi_{mc} = 0$, where

$$\pi_{mc} = \sum_n \{\int_{V_n}[(1/2)S_{ijkl}\dot{\sigma}_{ij}\dot{\sigma}_{kl} + \dot{\varepsilon}_{ij}{}^c\dot{\sigma}_{ij}]\,dV - \int_{\partial V_n}\dot{T}_i\dot{u}_i\,dS + \int_{S_{\sigma_n}}\dot{\bar{T}}_i\dot{u}_i\,dS\} \quad (2)$$

and ∂V_n is the entire boundary of the nth element. The displacements u_i are equal to $\bar{u}_i$ along S_{u_n}. The modified complementary principle leads to the assumed stress hybrid model which for the ordinary linear elastic analysis is again a matrix displacement method.

III. Creep Behavior under Multiaxial Loading Conditions

If the yield condition of a material can be expressed as

$$F(\sigma_{ij}) - \bar{\sigma} = 0 \quad (3)$$

where $\bar{\sigma}$ is the equivalent stress, the creep strain components are given by

$$\dot{\varepsilon}_{ij}{}^c = (\partial F/\partial\sigma_{ij})\dot{\bar{\varepsilon}}^c \quad (4)$$

Here $\dot{\bar{\varepsilon}}^c$ is the equivalent creep strain rate given by

$$\dot{\bar{\varepsilon}}^c = (2/3)^{1/2}(\dot{\varepsilon}_{ij}{}^c\dot{\varepsilon}_{ij}{}^c)^{1/2} \quad (5)$$

For steady-state creep; the creep strain rate is only a function of stress amplitude and temperature. For example under a constant temperature, the creep behavior may often be represented by a power law such as

$$\dot{\bar{\varepsilon}}^c = \dot{\varepsilon}_0(\bar{\sigma}/\lambda)^n \quad (6)$$

where, $\dot{\varepsilon}_0$, n, and λ constants for a given temperature.

For transient creep under the time-hardening rule, the creep strain rate is a function of stress amplitude and time. Under a corresponding power rule, the creep behavior may be represented by

$$\dot{\bar{\varepsilon}}^c = \dot{\varepsilon}_0 f(t)(\bar{\sigma}/\lambda)^n \quad (7)$$

IV. Finite Element Formulations

In the finite element formulation it is assumed for simplicity that the body forces $\bar{F}_i$ are absent and $u_i = \bar{u}_i$ along S_{u_n}. In that case, the formulations under both Eqs. (1) and (2) can be treated in a similar fashion. In such formulations the stresses are represented by

$$\boldsymbol{\sigma} = \mathbf{P}\boldsymbol{\beta} \quad (8)$$

where $\boldsymbol{\beta}$ are stress parameters. For the Hellinger-Reissner principle, the stresses need not satisfy the equilibrium conditions and may be either stress parameters which are independent for different elements or nodal values of stress components which are in common at the interelement boundary nodes. For the complementary energy principle, of course the stresses must satisfy the equilibrium conditions and $\boldsymbol{\beta}$ are independent for different elements. The tractions at the element boundary are related to the assumed stress distribution, they can be expressed as

$$\mathbf{T} = \mathbf{R}\boldsymbol{\beta} \quad (9)$$

The displacements in each element are then represented by interpolation functions and the generalized displacements $\mathbf{q}$ at a finite number of boundary nodes,

$$\mathbf{u} = \mathbf{L}\mathbf{q} \quad (10)$$

Under Eq. (1), $\mathbf{L}$ refers to interpolation functions over the element, while under Eq. (2) it is applied to the surface of the element.

By representing $\partial F/\partial\sigma_{ij}$ in matrix form by

$$\mathbf{F}_\sigma = \{\partial F/\partial\sigma_{11}, \ldots, \partial F/\partial\sigma_{13}\} \quad (11)$$

the rates of creep strain components $\dot{\varepsilon}_{ij}{}^c$ for steady-state creep behavior can be written as

$$\dot{\boldsymbol{\varepsilon}}^c = \dot{\varepsilon}_0(\bar{\sigma}/\lambda)^n\mathbf{F}_\sigma \quad (12)$$

Similar relations can be obtained for transient creep behavior under the time-hardening rule.

The matrix $\mathbf{F}_\sigma$ can be expressed in the form of

$$\mathbf{F}_\sigma = \boldsymbol{\sigma}^T\boldsymbol{\phi} \quad (13)$$

For example under the Huber-Mises-Hencky criterion when

$$\boldsymbol{\sigma} = \{\sigma_x\,\sigma_y\,\sigma_z\,\sigma_{xy}\,\sigma_{yz}\,\sigma_{xz}\} \quad (14)$$

$$\boldsymbol{\phi} = \frac{1}{\bar{\sigma}}\begin{bmatrix} 1 & -1/2 & -1/2 & 0 & 0 & 0 \\ -1/2 & 1 & -1/2 & 0 & 0 & 0 \\ -1/2 & -1/2 & 1 & 0 & 0 & 0 \\ 0 & 0 & 0 & 3/2 & 0 & 0 \\ 0 & 0 & 0 & 0 & 3/2 & 0 \\ 0 & 0 & 0 & 0 & 0 & 3/2 \end{bmatrix} \quad (15)$$

Thus the matrix $\mathbf{F}_\sigma$ may also be written as $\boldsymbol{\beta}^T\mathbf{P}^T\phi$ and both $-\pi_R$ and π_{mc} can be written as

$$\pi = \sum_n [(1/2)\dot{\boldsymbol{\beta}}\mathbf{H}_n\dot{\boldsymbol{\beta}} + \boldsymbol{\beta}^T\mathbf{M}_n\dot{\boldsymbol{\beta}} - \dot{\boldsymbol{\beta}}^T\mathbf{G}_n\dot{\mathbf{q}} + \dot{\mathbf{q}}^T\dot{\mathbf{Q}}_n] \quad (16)$$

where

$$\mathbf{H}_n = \int_{V_n} \mathbf{P}^T \mathbf{S} \mathbf{P}\, dV$$
$$\mathbf{Q}_n = \int_{S_{\sigma_n}} \mathbf{L}^T \mathbf{R}\, dS$$
$$\mathbf{G}_n = \begin{cases} \int_{V_n} \mathbf{P}^T \mathbf{B}\, dV; & \text{under Eq. (1)} \\ \int_{\partial V_n} \mathbf{R}^T \mathbf{L}\, dS; & \text{under Eq. (2)} \end{cases} \tag{17}$$

and for the steady-state creep,

$$\mathbf{M}_n = \dot{\varepsilon}_0 \int_{V_n} (\bar{\sigma}/\lambda)^r \mathbf{P}^T \boldsymbol{\phi} \mathbf{P}\, dV \tag{18}$$

Here $\mathbf{B}$ involves derivatives of $\mathbf{L}$ according to the strain displacement relation. The equivalent stress $\bar{\sigma}$ can be expressed in terms of σ, and hence also in terms of $\boldsymbol{\beta}$.

Since, in general, both $\boldsymbol{\beta}$ and $\mathbf{q}$ may refer to common nodes, it is required to assemble the matrices $\mathbf{H}_n$, $\mathbf{M}_n$, $\mathbf{G}_n$, and $\mathbf{Q}_n$ into corresponding global matrices, $\mathbf{H}$, $\mathbf{M}$, $\mathbf{G}$, and $\mathbf{Q}$; i.e.,

$$\pi = (1/2)\dot{\boldsymbol{\beta}}^T \mathbf{H} \dot{\boldsymbol{\beta}} + \dot{\boldsymbol{\beta}}^T \mathbf{M} \dot{\boldsymbol{\beta}} - \dot{\boldsymbol{\beta}}^T \mathbf{G} \dot{\mathbf{q}} + \dot{\mathbf{q}}^T \mathbf{Q} \tag{19}$$

In applying Eq. (2), of course, there will be no coupling between $\boldsymbol{\beta}$ matrices in different elements, hence $\mathbf{H}$, $\mathbf{M}$, and $\mathbf{G}$ are simply super diagonal matrices. The variation principle thus leads to the following system of equations

$$\begin{bmatrix} \mathbf{H} & -\mathbf{G} \\ -\mathbf{G}^T & \mathbf{O} \end{bmatrix} \begin{bmatrix} \dot{\boldsymbol{\beta}} \\ \dot{\mathbf{q}} \end{bmatrix} = \begin{bmatrix} -\mathbf{M}(\boldsymbol{\beta})\boldsymbol{\beta} \\ -\dot{\mathbf{Q}} \end{bmatrix} \tag{20}$$

or

$$\begin{bmatrix} \dot{\boldsymbol{\beta}} \\ \dot{\mathbf{q}} \end{bmatrix} = \begin{bmatrix} \mathbf{H} & -\mathbf{G} \\ -\mathbf{G}^T & \mathbf{O} \end{bmatrix}^{-1} \begin{bmatrix} -\mathbf{M}(\boldsymbol{\beta})\boldsymbol{\beta} \\ -\dot{\mathbf{Q}} \end{bmatrix} \tag{21}$$

This is a system of first-order nonlinear differential equations. With the initial conditions for $\boldsymbol{\beta}$ and $\mathbf{q}$ obtained by a linear elastic solution, Eq. (21) can be solved by many numerical methods.

References

[1] Percy, J. H., Loden, N. A., and Navaratna, D. R., "A Study of Matrix Analysis Methods for Inelastic Structures," RTD-TDR-63-4032, Oct. 1963, Air Force Flight Dynamics Lab., Wright-Patterson Air Force Base, Ohio.

[2] Lansing, W., Jensen, W. R., and Falby, W., "Matrix Analysis Methods for Inelastic Structures," *Proceedings of the First Conference on Matrix Methods in Structural Mechanics*, AFFDL-TR-66-80, Air Force Flight Dynamics Lab., Wright-Patterson Air Force Base, Ohio, pp. 605–633, 1965.

[3] Greenbaum, G. A. and Rubinstein, M. F., "Creep Analysis of Axisymmetric Bodies," *Nuclear Engineering and Design*, Vol. 7, 1968, pp. 379–397.

[4] Goodall, I. W. and Chubb, E. J., "Creep of Large Thin Plates with Central Circular Holes Subjected to Biaxial Edge Tractions," *Nuclear Engineering and Design*, Vol. 12, 1970, pp. 89–96.

[5] Sutherland, W. H., "AXICRP—Finite Element Computer Code for Creep Analysis of Plane Stress, Plane Strain and Axisymmetric Bodies," *Nuclear Engineering and Design*, Vol. 11, 1970, pp. 260–285.

[6] Chang, T. Y. and Rashid, Y. R., "Non-linear Creep Analysis at Elevated Temperature," *Proceedings of the First International Conference on Structural Mechanics in Reactor Technology*, compiled by T. A. Jaeger, Berlin, Vol. 6, Pt. L, 1971, pp. 271–291.

[7] Branca, T. R. and Boresi, A. P., "Creep of a Uniaxial Metal Composite Subjected to Axial and Normal Lateral Loads," *Proceedings of the First International Conference on Structural Mechanics in Reactor Technology*, compiled by T. A. Jaeger, Berlin, Vol. 6, Pt. L, 1971, pp. 109–131.

[8] Cyr, N. A. and Teter, R. D., "Finite-element Elastic-Plastic Creep Analysis of Two-dimensional Continuum with Temperature Dependant Material Properties," *Computers and Structures*, Vol. 3, 1973, pp. 849–863.

[9] Sanders, J. L., McComb, H. G., Jr., and Schlechte, F. R., "A Variational Theorem for Creep with Applications to Plates and Columns," Rept. 1342, 1968, NACA.

[10] Pian, T. H. H., "On the Variational Theorem for Creep," *Journal of Aerospace Sciences*, Vol. 24, 1968, pp. 846–847.

[11] Pian, T. H. H., "Creep Buckling of Curved Beam under Lateral Loading," *Proceedings of the 3rd U.S. National Congress of Applied Mechanics, ASME*, 1958, pp. 649–654.

[12] Pian, T. H. H. and Tong, P., "Basis of Finite Element Methods for Solid Continua," *International Journal of Numerical Methods in Engineering*, Vol. 1, 1969, pp. 3–28.

[13] Pian, T. H. H., Tong, P., Luk, C. H., and Spilker, R. L., "Elastic-plastic Analysis by Assumed Stress Hybrid Model," *Proceedings of the 1974 International Conference on Finite Element Methods in Engineering*, ed. by V. A. Pulmano and A. P. Kabaila, The Univ. of New South Wales, Kensington, N.S.W., Australia, Aug. 1974, pp. 419–434.

Laser Anemometer Measurements of Surface Pressure Distributions

S. J. BARKER* AND H. W. LIEPMANN†

California Institute of Technology, Pasadena, Calif.

I. Introduction

THE forces exerted upon a moving solid body in incompressible flow can always be obtained from velocity measurements on a suitable contour around the body. In particular, the surface pressure distribution can be deduced from velocity measurements taken on a contour just outside of a thin boundary layer. According to boundary-layer theory, the static pressure change across a thin boundary layer is of order $(\delta/l)^2$, where δ is the boundary-layer thickness and l is the length of the body. The x-momentum equation outside of the boundary layer is $U(dU/dx) = -(1/\rho)\, dp/dx$, which can be integrated to $p + \frac{1}{2}\rho U^2 = \text{constant}$ for the incompressible case. The surface pressure coefficient, defined as $c_p = (p - p_o)/\frac{1}{2}\rho U_o^2$, is then given by $c_p = 1 - (U/U_o)^2$. The error in this approximation to the surface pressure is of order $(\delta/l)^2$.

The present technique for measuring surface pressure distributions in wind or water tunnels requires the construction of models with many small static pressure taps in surfaces of interest. Such models are expensive and very difficult to build. The laser-Doppler velocimeter technique provides for the first time a convenient method of measuring velocities directly without any interference, and hence suggests a very attractive alternative for measuring pressure distributions on airfoil and hydrofoil sections. The application to hydrofoils is particularly attractive because the construction of these very thin sections with a sufficient number of pressure taps is often impractical. At the same time, the laser-Doppler technique is most easily used in water.

II. Experimental Technique

An experimental test of the feasibility of this method has been conducted in the Caltech High Speed Water Tunnel. This tunnel, described in Ref. 1, has a two-dimensional test section for testing 6 in. span hydrofoil models at velocities up to 85 fps. The models are cantilever mounted on one wall of the test section, and the opposite wall is transparent. The laser-Doppler velocimeter (LDV) used for this test is one which has been developed at Caltech, and has been applied to a variety of hydrodynamic flows.[2,3] The LDV optics are mounted on a traversing system which can scan the flowfield near the surface of a two-dimensional model and position the center of the measuring volume to within 0.001 in. Since this LDV operates in the forward scatter reference beam mode,[2] the mounting plate of the hydrofoil model has to be made of a specular reflecting material. In this way, the reference beam and forward scattered Doppler shifted light are reflected off the mounting plate, back out through the test section window and into the photodetector (see Fig. 1).

Received May 17, 1974; revision received July 29, 1974.

Index categories: Aircraft Aerodynamics; Hydrodynamics; Boundary Layers and Convective Heat Transfer—Turbulent.

* Assistant Professor, Department of Mechanics and Structures, University of California at Los Angeles.

† Director, Graduate Aeronautical Laboratories. Fellow AIAA.